OPEN ACCESS
Freely Available Online

JOURNAL OF HEMATOLOGY AND ONCOLOGY RESEARCH
ISSN NO: 2372-6601

Research Article

DOI: 10.14302/issn.2372-6601.jhor-19-3092

Monitoring Mast Cell Populations in Waldenström's Macroglobulinemia: A Xenotransplantation Study

Nikistratos Siskos[1], Chryssa Bekiari[1], Theophilos Poutahidis[2], Alexandros Chadras[2], Anastasia S. Tsingotjidou[1,*]

[1]Laboratory of Anatomy, Histology and Embryology, Faculty of Veterinary Medicine, School of Health Sciences, Aristotle University of Thessaloniki, Thessaloniki, GR-541 24, Greece

[2]Laboratory of Pathology, Faculty of Veterinary Medicine, School of Health Sciences, Aristotle University of Thessaloniki, Thessaloniki, GR-541 24, Greece

Abstract

Waldenström Macroglobulinemia (WM) is a B-cell lymphoproliferative disorder characterized mainly by uncontrolled accrual of M- immunoglobulin, secreted by malignant lymphoplasmatic cells. Mast cells interacting with malignant B-cells play an important role at the manifestation of the disease. Utilizing a previous xenotransplantation mouse model, this study evaluates long-term implant viability and quantifies distinct bone marrow mast cell populations along with their dynamics in non-WM and WM human bone implants.

Non-WM bone implants were obtained from the femoral head of adult humans undergoing hip arthroplasty or hemiarthroplasty, whereas WM human bone implants originated from bone biopsies obtained from the posterior iliac crest of patients with active WM. All bone particles were implanted intramuscularly in twenty-four NOD/SCID mice. Following 3, 4 or 8 months postoperatively, xenografts were removed and studied using special histological techniques to identify mature and immature mast cells.

Xenografts survived up to 8 months after implantation presenting normal cytoarchitecture (non-WM) or high-grade neoplastic infiltration and microresorption (WM bone biopsies). Statistical analysis of mast cell populations showed significant elevation regarding time progression and bone marrow microenvironment, thus suggesting the possible influence of malignant cells to the mast cell population in WM.

This study presents the extended survival of intramuscular implantation of human adult bone xenografts into NOD/SCID mice and provides additional information on the interaction between mast cells and malignant B-cells.

Corresponding author: Anastasia S. Tsingotjidou, Laboratory of Anatomy, Histology and Embryology, Faculty of Veterinary Medicine, School of Health Sciences, Aristotle University of Thessaloniki, Thessaloniki, GR-541 24, Greece. Email: astsing@vet.auth.gr

Citation: Nikistratos Siskos, Chryssa Bekiari, Theophilos Poutahidis, Alexandros Chadras, Anastasia S. Tsingotjidou (2019) Monitoring Mast Cell Populations in Waldenström's Macroglobulinemia: A Xenotransplantation Study. Journal of Hematology and Oncology Research - 3(3):9-20. https://doi.org/10.14302/issn.2372-6601.jhor-19-3092

Keywords: Waldenström Macroglobulinemia, mast cells, human adult bone, xenotransplantation, SCID mice

Running title: Mast cells in Waldenström's Macroglobulinemia

Received: Nov 16, 2019 **Accepted:** Dec 04, 2019 **Published:** Dec 11, 2019

Editor: Rohit Jain, Department of Pathology & Transfusion Medicine, Santokba Durlabhji Memorial Hospital, Jaipur, India .

Introduction

Waldenström Macroglobulinemia (WM) is a B-cell lymphoproliferative disorder characterized by the uncontrolled accumulation (predominantly in the bone marrow) of clonally related lymphoplasmacytic cells, which secrete M- immunoglobulin (IgM) [1-3]. With an age-adjusted incidence of 3.8 individuals per million per year, WM is a relatively rare condition [4]. Age, gender and ethnicity are factors that influence the development of the disease, with older males of Caucasian descent to be the group of people that are more affected by it. More specifically males are twice more likely to develop WM than females and the incidence on Caucasians has increased the past two decades [4, 5]. Waldenström Macroglobulinemia clinical manifestations are attributed either to the infiltration of the bone marrow (and other extramedullary sites), or to the elevated IgM serum levels [6, 7].

Despite progression in disease understanding, WM treatment remains symptom-oriented, while factors like patient's age and possible complications strongly influence the therapeutic protocol [6]. Furthermore, it is widely acceptable that WM remains incurable, while patients die of disease progression [8]. The need for better understanding of the disease mechanisms, has led to the development of several animal models. Most of them follow xenotransplantation methods: An immunocompromised mouse receives a human bone xenograft, free from WM, and malignant cells, either from *in vitro* cultures [8], or from fresh WM-bone biopsy implanted on the same animal [9]. Our study introduces the implantation of human bone xenograft with WM and the subsequent IgM production implying the development of the disease into the immunodeficient mice.

Arising from pluripotent hematopoietic stem cells of the bone marrow [10], mast cells are considered a hallmark of the disease, while their bone marrow excess serves as a supportive basis for pathologists [5, 11]. It has been further shown that mast cells interact with malignant cells in WM bone marrow, playing thus a major role in cancer growth, expansion, invasion, and migration [2, 3, 11-13].

In the present work, we investigated the interaction between mast and B-cells in the microenviroment of the tissue involved in the pathogenesis of WM by expanding an established WM animal model [9] .We hypothesize that by studying long-term mast cell population dynamics in non-WM and WM human bone xenografts, possible therapeutic schemes might be facilitated.

Materials and Methods

Animals

Twenty-four NOD/SCID mice (Charles River Laboratories, L'Arbresle Cedex, France) were used in the present study. Animals were housed in individually ventilated cages (IVC) at the biocontainment animal research facility of the Laboratory of Anatomy, Histology and Embryology of the Veterinary School (code number EL-54-BIOexp-24 of the Prefecture of Thessaloniki, Greece). All experimental procedures and protocols received the approval of the Veterinary Directorate of Thessaloniki, and were in accordance with the European Council Directive 2010/63/EU as well as the national and institutional guidelines for animal care.

Human Xenografts' Origin

Healthy bone fragments (3-5 × 4-6 mm in size) were obtained from the femoral head of adult humans (both gender) during hip arthroplasty or hemiarthroplasty [14]. Waldenström macroglobulinemia bone biopsies were obtained from the posterior iliac crest of patients with active WM during scheduled clinical visits [9]. All bone implant donors signed Institutional Review Board - approved informed consent forms.

Bone xenografts were implanted into the right or left hindlimb muscles of 6- to 8- week old mice . On the basis of xenograft origin, animals were divided into two groups: Animals receiving non-WM bone implants (n = 12) were assigned as the non-WM group. Rest animals (n = 12) were implanted with WM bone biopsies, consisting thus the WM group. Finally, mice were transcardially perfused 3 (n = 4), 4 (n = 5) or 8 months (n = 3) post implantation (p.impl.) of bone fragments, with 0.9% saline, followed by 4% paraformaldehyde solution (see flow chart). Other time points were also evaluated for comparison reasons (1-3 weeks, 1, 5 and 9 months p. impl.). For detailed experimental procedures please see reference 9.

Histology

At necropsy, bone xenografts were collected and

fixed in 4% paraformaldehyde solution for 24 hours. Following decalcification, grafts were processed routinely, embedded in paraffin, sectioned at 8μm and stained with haematoxylin & eosin (H&E). In order to further evaluate mature (MMC) and immature (IMC) mast cells, selected sections were treated overnight with either Toluidine Blue (pH=2.3) or Alcian Blue/Safranine, respectively. Mature mast cells contain mostly heparin and present metachromasia (due to densely packed sulphate groups) after low pH Toluidine Blue treatment, while IMC contain biogenic amines and stain positively with the Alcian Blue/Safranine technique.

Histopathology

For immunohistochemical evaluation of the malignant cells in the WM specimens (4% paraformaldehyde fixed, paraffin embedded, 8μm sectioned), a rabbit monoclonal antibody against c-kit (Cell Marque, Rocklin, CA) was used. Heat-induced antigen retrieval was performed with EDTA buffer, pH 8. Primary antibody binding was detected with goat anti-rabbit polymer HRP (ZytoChem Plus, Berlin, Germany). Color was developed with Ultravision DAB substrate-chromogen system (ThermoFisher Scientific/ Lab Vision), and tissues were counterstained with hematoxylin (For detailed experimental procedures please see reference 9).

Counting Mature and Immature Mast Cells

Regarding non-WM implants, mast cells were counted in up to four consecutive sections coming from 4 (MMC) or 1 (IMC)(3 months), 7 (MMC) or 3 (IMC)(4 months) and 6 (MMC) or 1(IMC)(8 months) randomly chosen slides (n=3 animals in total). In WM implants, mast cells were counted in up to nine consecutive sections coming from 7 (MMC) or 3 (IMC) (3 months), 10 (MMC) or 4 (IMC) (4 months) and 4 (MMC) or 1 (IMC) (8 months) randomly chosen slides (n=9 animals in total). In all instances, the whole implant was cut. In order to count mast cell populations, all sections were studied using gradually the ×10 and ×20 objectives. All cell-like, positively stained structures that presented a nuclear clearance were considered to be mast cells (MMC on Toluidine Blue and IMC on Alcian Blue/ Safranine sections) and were counted manually with a camera lucida. Finally, each section's area was calculated using image analysis system (Image ProPlus, version 6.1, Media Cybernetics) and mast cell population density was expressed as number-of-cells per square millimeter (mm^2).

Statistical Analysis

For data analysis the SPSS 22.0 statistical software was used. One-way ANOVA (Bonferroni post hoc analysis) and independent samples T-test were used for comparisons between groups. When homogeneity of variances was violated (Levene's test; $P< 0.05$) the non-parametric two-tailed Kruskal-Wallis was assessed for multiple comparisons, followed by the Mann-Whitney U test (two-tailed) for two-by-two comparisons. All results are expressed as mean ± S.E. Significance was set at $P< 0.05$.

Results

Human Bone Histology is Retained in Non-WM Implants Eight Months Following Intramuscular Implantation in NOD/SCID Mice.

Our results showed that all human bone histological characteristics were preserved long time following its implantantion into the mice. Following are the detailed results for every time period that the specimens were collected:

Three months: Bone medulla from non-WM implants, presented a rather restored histological image resembling healthy human bone marrow. Sites of fibrosis and necrosis tended to disappear. Cellularity was significantly restored while large adipocytes could be clearly observed. The newly formed bone grew further while newly encapsulated osteocytes (originating from osteoblasts) could be easily observed near the surface of bone trabeculae. Furthermore, the separation line between new and old osteoid was clearly distinct (Fig. 1A).

Four months: Non-WM implants had a similar histological appearance to these collected three months after implantation: Cellularity was restored, many large adipocytes were present, while necrotic sites could not be observed. The balance between osteosynthesis and osteolysis (bone remodeling) was rather shifted towards the synthetic direction since only new bone and osteoblast lineage cells were present along the surface of all observable bone trabeculae (Fig. 1B).

Eight months: Non WM implants presented a rather normal medullar histological profile: Vascular sinusoids scattered all through the marrow and small adipocytes separating the hematopoietic tissue into islets. Necrotic foci had disappeared but wave formed nuclei indicated

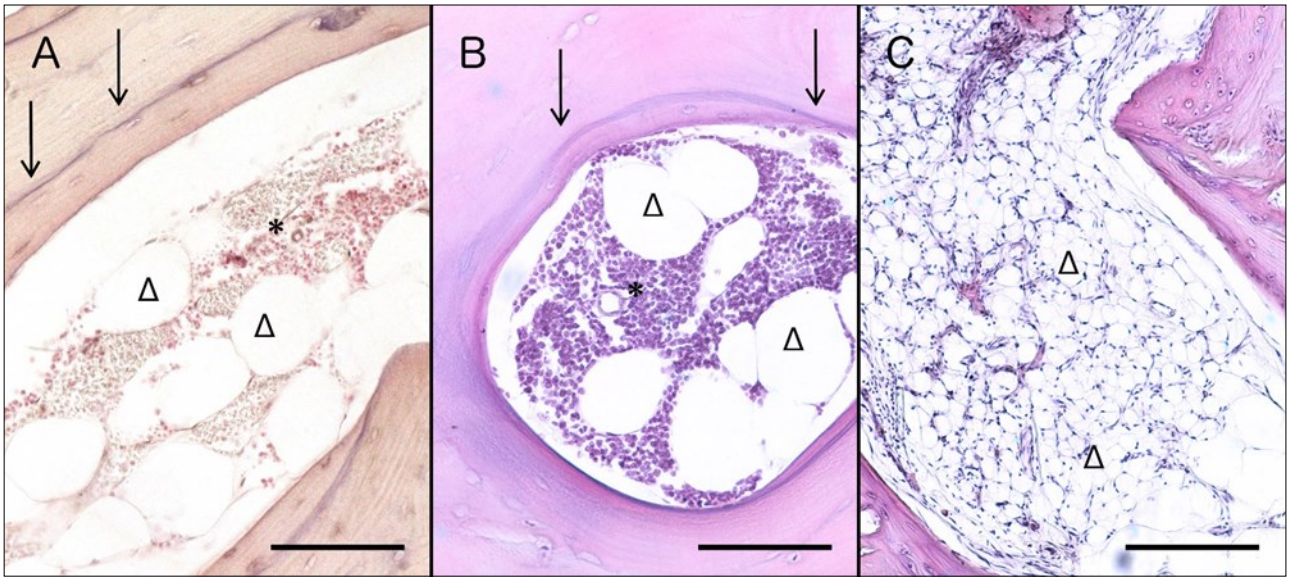

Figure 1. Histological evaluation of non-WM implants 3 (A), 4 (B) and 8 (C) months after implantation. Three months post implantation specimens (A) present restored cellularity and large adipocytes, while the sharp cement lines clearly separate old and new bone; H&E; Scale bar: 0.1mm. Four-month specimens (B) present a highly similar histological profile with 3 months, in terms of restored cellularity, large adipocytes and clear cement lines; H&E; Scale bar: 0.1mm. Eight months after surgery (C), bone marrow of xenografts present also restored cellularity and small adipocytes; H&E; Scale bar: 0.2mm. Cellularity is labelled with asterisks, adipocytes with triangles, and cement line with arrows.

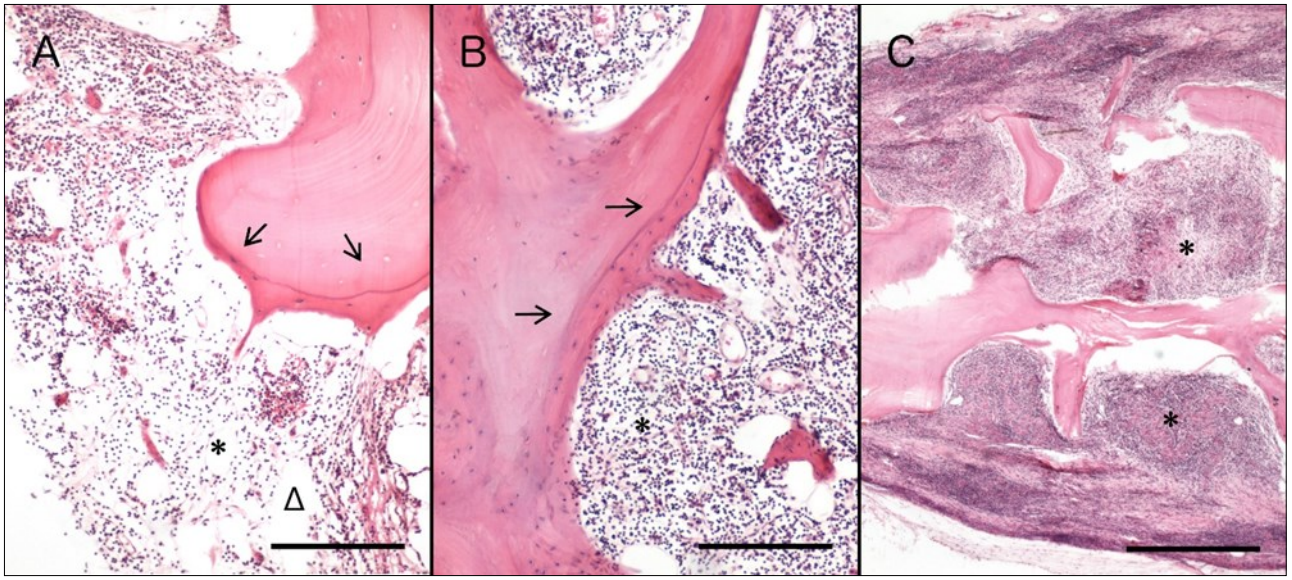

Figure 2. Histological evaluation of WM bone biopsies 3 (A), 4 (B) and 8 (C) months post implantation. Specimens collected three months after implantation (A) present infiltration of malignant cells, as well as adipocytes, while bone trabeculae appear thinned; H&E; Scale bar: 0.2mm. Four months after surgery (B), specimens present also thinned bone trabeculae and bone marrow infiltration by WM cells; H&E; Scale bar: 0.2mm. Biopsies extracted 8 months post implantation (C) also present resorptive lesions and high-grade infiltration by malignant cells; H&E; Scale bar: 0.5mm. Cellularity due to malignancy is labelled with asterisks, adipocytes with triangles, and cement line with arrows.

the presence of fibroblasts. New bone presented a similar histological profile with that appearing in xenografts collected four months after implantation (Fig. 1C).

WM Bone Biopsies Present High-Grade Malignant Cell Infiltration and Increased Bone Resorption Eight Months After Intramuscular Implantation in NOD/SCID Mice.

Our results showed that WM bone biopsies preserved all neoplastic characteristics along with their resorptive effects long time following their implantation into the mice. Following are the detailed results for every time period that the specimens were collected:

Three months: Bone marrow from WM bone biopsies was infiltrated mainly by small lymphocytes, plasmacytoid lymphocytes and plasma cells. Loose connective tissue septa divided bone marrow into distinctive departments, while few large adipocytes were present. Bone medulla from one animal however, presented large areas full of big adipocytes and smaller areas containing malignant cells. Newly encapsulated osteocytes may resemble osteosynthetic activity, but the presence of thinned trabeculae and large lacunae over bone surfaces indicated also active osteolysis (Fig. 2A).

Four months: WM bone biopsies of 4 months were also related with 3-month biopsies. Low-power microscopy revealed high cellularity, fibrotic foci and cells presenting condensed, highly basophilic nuclei. Malignant lymphocytes were the dominant cell population, followed by plasmacytoid lymphocytes and plasma cells. Finally, presence of large lacunae extending from the bone surface down to cement line level and thinned trabeculae (Fig. 2B), revealed that the remodeling equilibrium was highly shifted towards the lysis direction.

Eight months: WM bone biopsies presented high-grade cell infiltration, resembling to an active malignant procedure. Malignant B-cells and plasmacytoid lymphocytes dominated over the bone marrow (Fig. 2C), while areas featuring bundles of dense irregular connective tissue indicated high-grade fibrosis. Osteolysis was evident in a same manner like 4 months-after-implantation biopsies, except for one animal featuring hyaline cartilage that presented areas of undergoing endochondral ossification (data not shown).

Mast Cells are Present at the Human Bone Marrow Niche

The low pH of Tolouidine Blue staining results to metachromasia of the stained cells. For this reason, mature mast cells are displayed light purple-blue (Fig. 3A and B) effect that renders them easily recognizable from the other neighbouring cells of hematopoietic origin. Positive cells showed an elongated shape implying their location in interstitial regions [15].

Immature mast cells, on the other hand, stain positively with the Alcian Blue/Safranine technique due to their high concentration in biogenic amines giving them a blue color easily distinguishable from the red staining of the surrounding cells.

Change in the staining properties from blue to red implicates maturation of the mast cells when stained with the above-mentioned technique [15,16]. Our findings indicate the presence of mature mast cells (Fig. 3C) in proximity to the other bone marrow cells, whose nuclei are stained red from the Safranine.

Mast cells express the Kit receptor for the stem cell factor, which plays important role in regulating mast cell biology [15]. C-kit positive cells were found in the highly populated area of the bone marrow (Fig. 3D-F). C -kit staining in normal cells is located in plasma membrane; in diseased cells, it is found into their cytoplasm. Our findings show the staining to be mostly in the plasma membrane, but it is also found in the cytoplasm, implying possibly, the transition from one stage to the other.

Mast Cell Populations Elevate Along Time Progression, While WM Bone Biopsies Present More Mature and Immature Mast Cells than their Non-WM Counterparts.

Three months p.impl., non-WM implants presented 0.180±0.07 and 0.209±0.095, MMC/mm^2 and IMC/mm^2 respectively. One month later, at 4 months p.impl., 0.059±0.024 MMC/mm^2 and 0.443±0.120 IMC/ mm^2 could be observed, while at 8 months p.impl. 1.190±0.230 MMC/mm^2 and 2.594±0.801 IMC/mm^2 were counted (Diagr. 1A). Statistical analysis proved that populations of mast cells found at 8 months p. impl., were significantly increased as compared to their values at 3 (MMC, P= 0.003; IMC, P = 0.034) and 4 months p.impl. (MMC, P = 0.0001; IMC, P = 0.011); (Tables 1 and 2).

Simultaneous counting of the mast cell populations in the WM bone biopsies (Diagr. 1B)

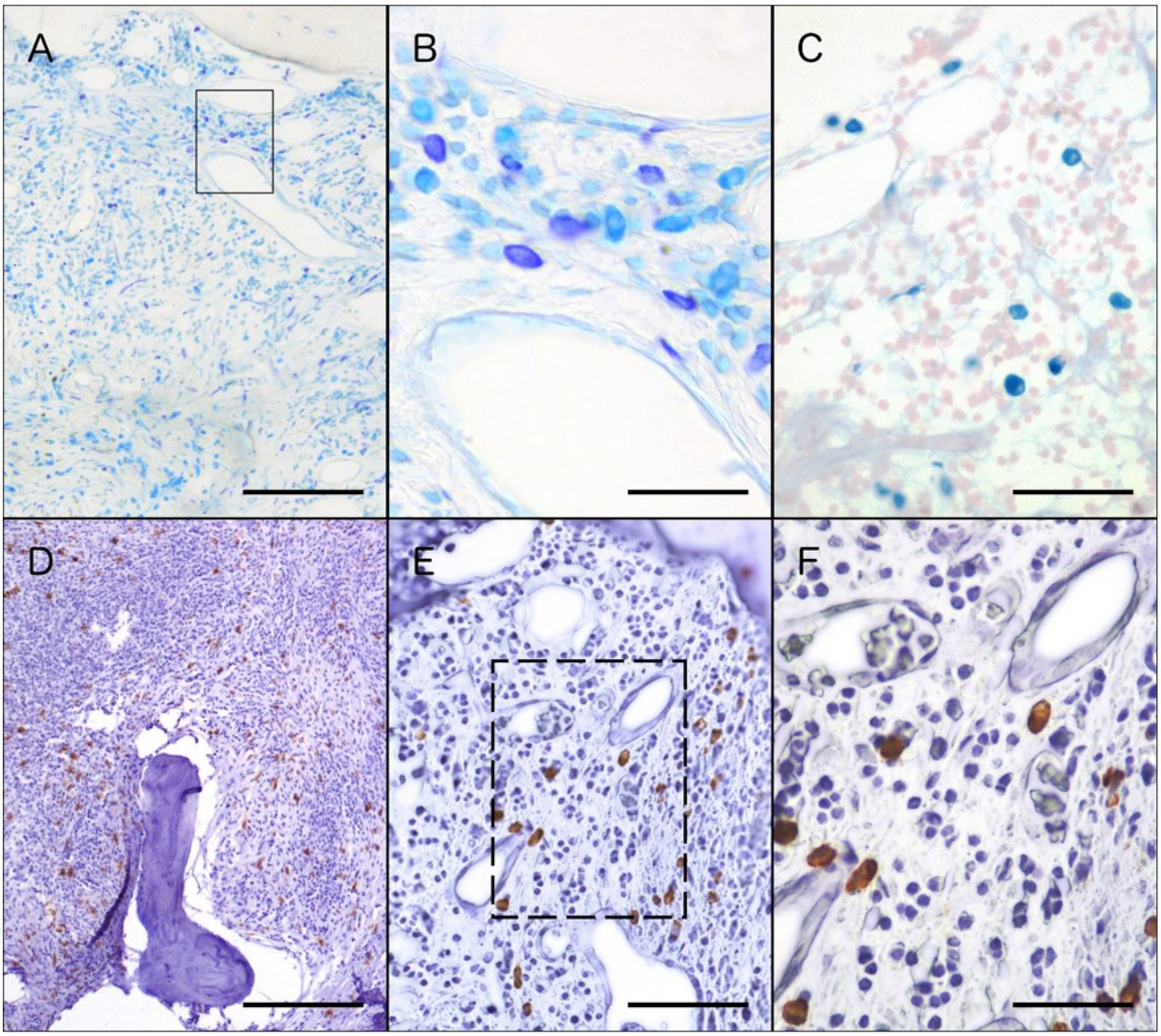

Figure 3. Histological (A-C) and immunohistochemical (D-F) staining of mast cells in WM biopsies.

Mast cells were identified using conventional histological staining (A-C) and immunohistochemical methods (E-G): Tolouidine Blue staining revealed mature mast cells in the bone marrow of the implanted WM bone (osteoid shown in 3A). They differ from their adjacent cells not showing metachromatic reaction (B represents the marked area of A). Immature mast cells are round Alcian blue stained cells (3C) in contrast to the Safranine stained cells of the marrow vicinity.

Mast cells were also detected with IHC against c-kit (D-F). Positive stained cells are shown in the bone marrow of diseased animals (F represents the dashed area of E). C-kit positive cells are dispersed all over the highly densed area of the bone marrow. Although they showed an accumulation of the reaction into the plasma membrane, c-kit staining is into their cytoplasm as well (3F). Scale bars represent 0.1 mm in A and E, 0.05 mm in C and F, 0.02 mm in B and 0.2 mm in D.

Table 1. MMC (TB stained) number over a period of 5 months

TB cells/mm² *(Mean ± SEM)*	**3 mos**	**4 mos**	**8 mos**	P
non-WM	0.180±0.07*	0.059±0.024*	1.190±0.230**	* 0.003 * 0.0001
WM	1.311±0.275*	5.567±0.711*	2.966±0.258**	* <0.0001 * 0.460
P	* 0.019	* <0.0001	** <0.0001	

Table 2. IMC (AS stained) number over a period of 5 months

AS cells/mm² *(Mean ± SEM)*	**3 mos**	**4 mos**	**8 mos**	P
non-WM	0.209±0.095*	0.443±0.120*	2.594±0.801**	* 0.034 * 0.011
WM	23.677±4.567*	43.921±3.671*	59.689±3.118**	* <0.0001 * 0.085
P	*0.024	*<0.0001	** <0.0001	

revealed that their number increases over time not only in the non-WM but in the WM implants as well (3 months p.impl.:1.311±0.275 MMC/mm^2 and 23.677±4.567 IMC/mm^2; 4 months p.impl.: 5.567±0.711 MMC/mm^2 and 43.921±3.671 IMC/mm^2;8 months p.impl.: 2.966±0.258 MMC/mm^2 and 59.689±3.118 IMC/mm^2). Regarding MMC, statistical analysis proved significant difference between 3 and 4 months p.impl. (P = 0), and 3 and 8 months p.impl.(P = 0), while no significant difference occurred between 4 and 8 months p.impl. (P = 0.460). At the same time, numerical changes in the populations of IMC over time seem to follow the same pattern (3 and 4 months p.impl.,P = 0.003; 3 and 8 months p.impl., P = 0; 4 and 8 months p.impl., P = 0.085).

Comparing MMC populationsin the non-WMand WM implants (Diagr. 1C), they were found to be significantly higher in the WM bone biopsies at all examined time points (3 months p.impl.,P = 0.019; 4 months p.impl., P = 0; 8 months p.impl., P = 0), while the same was revealed for IMC populations (Diagr. 1D), as well (3 months p.impl., P = 0.024; 4 months p.impl., P = 0; 8 months p.impl., P = 0).

Discussion

The microenvironment of cancer cells plays pivotal role in the progress of every malignancy. In Waldenström's Macroglobulinemia, bone marrow niche is this specific area where interactions between malignant B cells and the neighboring cells take place. Factors like interleukins and cytokines are expressed by bone marrow cells, including endothelial and stromal cells [17]. Mast cells, are among others, capable of influencing malignant bone marrow cells. Great research has been done on the relationship between mast and malignant B-cells in WM. Their bidirectional interactions are considered at least significant in the pathogenesis and further expansion of the disease [17]. Mast and B-cells "communicate" utilizing various ligand-receptor interactions. Mast cells for example, express tumor necrosis factor family ligand CD154, which binds on malignant WM cell surface molecule CD40, inducing proliferation of the latest [11]. Malignant B-cells on the other hand, utilize CD27/CD70 interactions in order to stimulate CD154 expression on neighboring mast cells [3, 12]. Further examples include CCL3, APRIL, BLYS and CD52 interactions [3, 11-13], revealing the

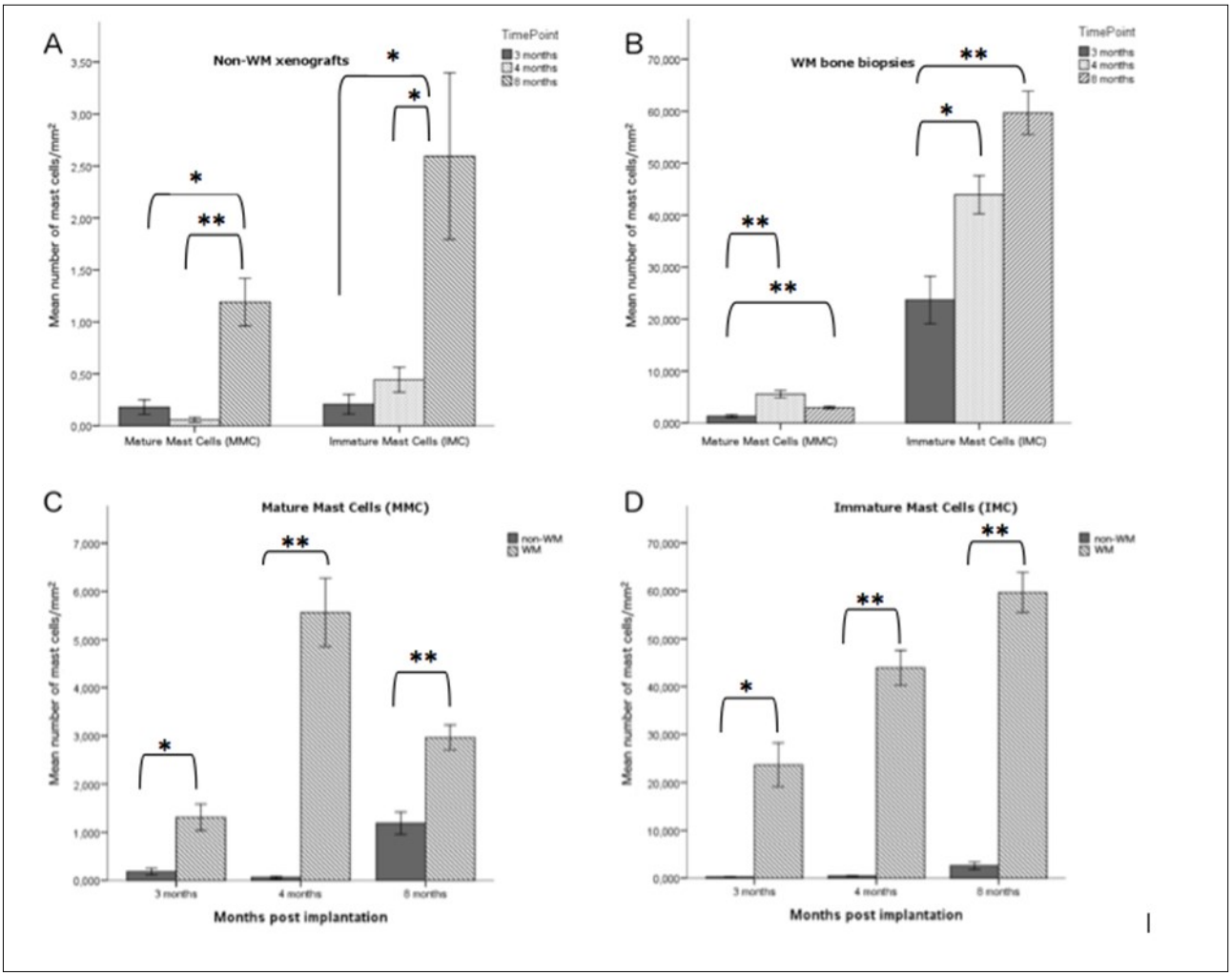

Diagram 1.

A and **B** diagrams represent the mean number of the MMC and IMC counted cells/mm^2 over time in the non-WM bone fragments (A) and WM bone biopsies (B). * P< 0.05, ** P< 0.001

C and **D** Comparative evaluation of MMC (C) and IMC (D) counted cells/mm^2 over time in the non-WM bone fragments and WM bone biopsies. * P< 0.05, ** P< 0.001

In all three time points that were checked (3, 4 and 8 months post implantation) the mean number of counted cells/mm^2 (both Tolouidine Blue and Alcian Blue/Safranine stained cells) was higher in the animals implanted with WM bone biopsies (C and D).

importance of the aforementioned "cross-talk". Jalali and Ansell (2018) conclude that the increased number of mast cells promote malignant cell growth through BAFF/ APRIL/CD70/CD40 L signaling.

The above-mentioned involvement of mast cells in the pathogenesis of the disease was demonstrated with the expression of mast cell tryptase in fetal bone marrow sections following implantantion of the fetal bone into immunodeficient mice [8], the expression of CD52 on human Mast Cells (MCs) and WM bone marrow lymphoplasmacytic cells implying their interaction to the pathogenesis of the disease [2], the corroboration in human patients of CD154-CD40 signaling providing the framework for therapeutic targeting of MC and MC-WM cell interactions in WM [11], while Terpos et al. (2011) have demonstrated the expression of CCL3 in neoplastic cells in 67 WM patients stating that this chemokine is also a chemoattracting factor for mast cells. The publication of Ho et al. (2008) demonstrated the injection of an established WM cell line (BCWM.1 cell line) into SCID mice suggesting a functional role for sCD27 in WM.

To our knowledge this is the first study to highlight and describe "kinetics" of distinct mast cell populations in Waldenström's Macroglobulinemia into the real environment of a bone biopsy from WM patients and their subsequent implantation into immunodeficient mice. More specifically, the possible participation of mast cells in WM was studied in the bone marrow niche of WM patients implanted intramuscularly into the hindlimbs of NOD/SCID mice. Control non-WM bone fragments were also implanted into the above-mentioned mice.

Concerning the site of grafting we have presented in our previous studies successful intramuscular implantation of human bone particles into mice [14]. Many researchers have implanted human tissues subcutaneously [8, 19-21, 24]. This approach might be technically easier or better in terms of animal welfare, but to our belief, it lacks adequate oxygenation. It is widely acceptable that utilization of an oxygen-rich, well-perfused tissue is a more suitable environment for a graft to thrive. Thus, hind limb muscles were used as cradles for both non-WM and WM xenografts at this study. One study has also shown the intramuscular implantation of technically produced particles into mice to study bone formation [29].

Although, xenografts from other species (e.g. rabbits) have been used successfully in the past [25], the use of consent-obtained human tissues not only does not raise ethical questioning, but it is also one step closer to reproducing the human disease. Another long-standing debate exists over the use of fetal or adult tissues. Although there is evidence on special chemotactic agents in fetal human bone [26], the fetal bone marrow dynamics are quite different than the adult one. Using adult xenografts, a more precise recapitulation of the disease is attempted, not only in the context of WM, but also in the study of osteotropism of primary malignant tumors such as prostate and/or breast [21, 30, 31].

One of the limitations of our study is the inclusion of femoral head bone fragments as controls while our experimental specimens are from iliac crest bone biopsies. Although macro- and micro- site specific variations of bone physiology have been reported [32, 33], we believe that our findings are valid because they represent basic bone homeostatic mechanisms.

For over two decades bone among other human tissues has been implanted into immunodeficient mice for studying different human disease related issues [27, 28]. Since then, this animal model (of human bone implantation into immunodeficient mice) has been used widely, mainly for the study of malignant cell osteotropism [30, 31]. One successful implementation of this model is the development of WM disease [9]. On this context, it was shown that healthy and WM adult human bone xenografts implanted either subcutaneously or intramuscularly in immunocompromised mice, are viable up to five months [9, 14, 18-22]. In the present study, the xenograft survival period was followedup to 8 months post-implantation. Detailed histological analysis of non-WM specimens indicates that both normal bone marrow histology and normal bone remodeling are completely restored (Fig. 1). In a same manner, WM biopsies' viability was proved by the high-grade infiltration of bone marrow with malignant cells (Fig. 2). Furthermore, the presence of thinned bone trabeculae and large lacunae over wide areas of bone, indicate microresorptive lesions, in accordance with previous findings [23]. This outcome gives the opportunity to evaluate the disease through a substantial period of time

thus allowing us to follow possible changes indicative of the pathogenesis of the disease, and/or better predict the effects of pharmaceutical agents.

To our knowledge the present study is the first one to monitor mast cell populations by detecting their maturity using conventional histological stains. Although more animals need to be examined (especially at some later time points) there is an obvious tendency for increased mast cell populations both in WM and non-WM groups. More specifically, our results indicate that populations of MMC and IMC show increasing pattern over time both in non-WM and WM xenografts. However, in the non-WM implants, MMC population shows its major increase between 4 and 8 months p. impl., while in the WM bone biopsies the increase is observed earlier, between 3 and 4 months p. impl., possibly indicating an accelerated mast cell production and maturation rate in the WM microenvironment compared to the non-WM one. These findings supplement existent aforementioned research, emphasizing mast cells' teleological role in WM pathogenesis and significance of mast cell - malignant B-cell interactions [3, 11, 13].

The positive c-kit stained mast cells (Fig. 3) verify not only their existence in the microenvironment of the diseased bone marrow but show their density as well. Although CD117 (c-kit) staining is also expressed on immature hematopoietic progenitor cells [15], our histological results in combination with the immunohistochemical ones indicate the same population of mast cells.

To Summarize, the Present Study Includes:

1. the cytoarchitecture presentation of WM and non-WM bone fragments for a long time period
2. mature and immature mast cells staining with conventional histological stains
3. c-kit immunohistocemical staining of the real microenvironment of the disease
4. adjacency of mast cells with other bone marrow cells into the real microenvironment
5. comparison with the non-WM specimens

Further research will elucidate the contribution of these cellular interactions to the pathogenesis and/or treatment of the disease.

Conclusion

Although other researchers have demonstrated the involvement of mast cells in the progress of WM previously, this study is the first one to demonstrate the existence of these cells in close adjacency with the cells of the bone marrow niche, where malignant B-cells reside. The specific interaction was visulaized in an animal model developed with the implantation of WM bone biopsies of human origin, and their subsequent monitoring for a long-lasting time period (up to 8 months). This finding can be a useful tool in future studies for clarifying additional structures responsible for the "crosstalk" between mast and malignant cells and hence developing new treatments for the disease.

Abbreviations

AB = Alcian Blue/Safranine

IgM = immunoglobulin-M

IMC = immature mast cells

MMC = mature mast cells

mos = months

NOD/SCID = Non-Obese Diabetic/Severe Combined ImmunoDeficient

p. impl. = post implantation

TB = Tolouidine Blue

wk(s) = week(s)

WM = Waldenström's Macroglobulinemia

Author's Contribution

AT performed the experiments, NS performed all the histological staining, NS and CB analyzed the data, TP and AC performed the immunohistochemistry of the tissue, NS and CB contributed to the writing of the manuscript. All authors read and approved the final manuscript.

Acknowledgements

This research was supported by the International Waldenström's Macroglobulinemia Foundation (IWMF) with codes of AUTh Research Committee: 82259 and 21962. We thank Dr. C. E. Emmanouilides for his scientific input to the grant proposal and Prof. P. Givissis for providing us with the human bone specimens.

References

1. Castillo JJ, Ghobrial IM, Treon SP (2015) Biology,

Prognosis, and Therapy of Waldenström Macroglobulinemia. In: Evans AM and Blum KA (eds) Non-Hodgkin Lymphoma. Springer International Publishing, Switzerland, pp 177-195, doi: 10.1007/978-3-319-13150-4_7

2. Terpos E, Tasidou A, Kastritis E, Eleftherakis-Papaiakovou E, Gavriatopoulou M, Migkou M, Dimopoulos MA (2009) Angiogenesis in Waldenström's Macroglobulinemia. Clinical Lymphoma and Myeloma 9:46-49. doi: 10.3816/CLM.2009.n.011
3. Santos DD, Hatjiharissi E, Tournilhac O, Chemaly MZA, Leleu X, Xu L, Patterson C, Branagan AR, Manning RJ, Ho AW, Hunter ZR, Dimmock EA, Kutok JL, Churchill WH, Castells MC, Tai Y-T, Anderson KC, Treon SP (2006) CD52 Is Expressed on Human Mast Cells and Is a Potential Therapeutic Target in Waldenström's Macroglobulinemia and Mast Cell Disorders. Clinical Lymphoma and Myeloma 6: 478-483
4. Gertz MA (2012) Waldenström Macroglobulinemia: 2012 update on diagnosis, risk stratification, and management. Am J Hematol 87:504-510. doi: 10.1002/ajh.23192
5. Treon SP, Hunter ZR, Castillo JJ, Merlini G (2014) Waldenström Macroglobulinemia. Hematol Oncol Clin North Am 28:945-970. doi: 10.1016/j.hoc.2014.06.003
6. Sahin I, Leblebjian H, Treon SP, Ghobrial IM (2014) Waldenström Macroglobulinemia: from biology to treatment. Expert Rev Hematol 7:157-168. doi: 10.1586/17474086.2014.871494
7. Janz S (2013) Waldenström Macroglobulinemia: Clinical and Immunological Aspects, Natural History, Cell of Origin, and Emerging Mouse Models. ISRN Hematology 2013, Article ID 815325, 25 pages. doi: 10.1155/2013/815325
8. Tassone P, Neri P, Kutok JL, Tournilhac O, Santos DD, Hatjiharissi E, Munshi V, Venuta S, Anderson KC, Treon SP, Munshi NC (2005) A SCID-hu in vivo model of human Waldenström Macroglobulinemia, Blood 106:1341-1345. doi: 10.1182/blood-2004-11-4477
9. Tsingotjidou AS, Emmanouilidis CE, Siotou E, Poutahidis T, Xagorari A, Loukopoulos P, Sotiropoulos D, Bekiari C, Doulberis M, Givissis P, Fassas A, Anagnostopoulos A (2009) Establishment of an animal model Waldenström's macroglobulinemia. Exp Hematol 37:469-476. doi: 10.1016/j.exphem.2008.12.007
10. Metcalfe DD, Baram D, Mekori YA (1997) Mast Cells. Physiol Rev 77:1033-1079
11. Tournilhac O, Santos DD, Xu L, Kutok J, Tai Y-T, Le Gouill S, Catley L, Hunter Z, Branagan AR, Boyce JA, Munshi N, Anderson KC, Treon SP (2006) Mast cells in Waldestrom's macroglobulinemia support lymphoplasmacytic cell growth through CD154/CD40 signaling. Ann Oncol 17:1275-1282. doi: 10.1093/annonc/mdl109
12. Ho AW, Hatjiharissi E, Ciccarelli BT, Branagan AR, Hunter ZR, Leleu X, Tournilhac O, Xu L, O'Connor K, Manning RJ, Santos DD, Chemaly M, Patterson CJ, Soumerai JD, Munshi NC, McEarchem JA, Law C-L, Grewal IS, Treon SP (2008) CD27-CD70 interactions in the pathogenesis of Waldenström macrobulinemia. Blood 112:4683-4689. doi: 10.1182/blood-2007-04-084525
13. Terpos E, Tasidou A, Eleftherakis-Papaiakovou E, Christoulas D, Gavriatopoulou M, Gkotzamanidou M, Roussou M, Kastritis E, Papadaki T, Dimopoulos MA (2011) Expression of CCL3 by Neoplastic Cells in Patients with Waldenström's Macroglobulinemia: An Immunohistochemical Study in Bone Marrow Biopsies of 67 Patients, Clinical Lymphoma Myeloma and Leukemia 11:15-117. doi: 10.3816/CLML.2011.n.024
14. Tsingotjidou AS, Zotalis G, Jackson KR, Sawyers C, Puzas JE, Hicks DG, Reiter R, Lieberman JR (2001) Development of an animal model for prostate cancer cell metastasis to adult human bone. Anticancer Res 21:971-8
15. Ribatti D (2018) The Staining of Mast Cells: A Historical Overview. Int Arch Allergy Immunol. 176 (1):55–60.
16. Combs JW, Lagunoff D, Benditt EP (1965) Differentiation and proliferation of embryonic mast cells of the rat. J Cell Biol. Jun;25(3):577-592.
17. Jalali S, Ansell SM (2018) The Bone Marrow Microenvironment in Waldenström Macroglobulinemia. Hematol Oncol Clin North Am.

Oct;32(5):777-786. doi: 10.1016/j.hoc.2018.05.005

18. Roato I, Caldo D, Godio L, D'Amico L, Giannoni P, Morello E, Quarto R, Molfetta L, Buracco P, Mussa A, Ferracini R (2010) Bone invading NSCLC cells produce IL-7: mice model and human histologic data. BMC Cancer 10:12. doi: 10.1186/1471-2407-10-12
19. Yang W, Lam P, Kitching R, Kahn HJ, Yee A, Aubin JE, Seth A (2007) Breast Cancer Metastasis in a Human Bone NOD/SCID Mouse Model. Cancer Biol Ther 6:e1-e6. doi: 10.4161/cbt.6.8.4504
20. Kuperwasser C, Dessain S, Bierbaum BE, Garnet D, Sperandio K, Gauvin GP, Naber SP, Weinberg RA, Rosenblatt M (2005) A Mouse Model of Human Breast Cancer Metastasis to Human Bone, Cancer Res 65:6130-6138. doi: 10.1158/0008-5472.CAN-04-1408
21. Yonou H, Yokose T, Kamijo T, Kanomata N, Hasebe T, Nagai K, Hatano T, Ogawa Y, Ochiai A (2001) Establishment of a Novel Species- and Tissue-specific Metastasis Model of Human Prostate Cancer in Humanized Non-Obese Diabetic/Severe Combined Immunodeficient Mice Engrafted with Human Adult Lung and Bone, Cancer Res 61:2177-2182
22. Boynton E, Aubin J, Gross A, Hozumi N, Sandhu J (1996) Human Osteoblasts Survive and Deposit New Bone When Human Bone Is Implanted in SCID Mouse. Bone 18:321-326
23. Marcelli C, Chappard D, Rossi J-F, Jaubert J, Alexandre C, Dessauw P, Baldet P, Bataille R (1988) Histologic Evidence of an Abnormal Bone Remodelling in B-Cell Malignancies Other Than Multiple Myeloma. Cancer 62:1163-1170
24. Moreau JE, Anderson K, Mauney JR, Nguyen T, Kaplan DL, Rosenblatt M (2007) Tissue-Engineered Bone Serves as a Target for Metastasis of Human Breast Cancer in a Mouse Model. Cancer Res 67:10304-10308. doi: 10.1158/0008-5472.CAN-07-2483
25. Yata K, Yaccoby S (2004) The SCID-rab model: a novel in vivo system for primary human myeloma demonstrating growth of CD138-expressing malignant cells. Leukemia 18:1891-1897
26. Somerman MJ, Hotchkiss RN, Bowers MR, Termine J (1984) Comparison of fetal and adult human bone: Identification of a chemotactic factor in fetal bone. J Metab Bone Dis Relat Res 5:75-79. doi: 10.1016/0221-8747(83)90005-X
27. Sandhu JS, Boynton E, Gorczynski R, Hozumi N (1996) The use of SCID mice in biotechnology and as a model for human disease. Crit Rev Biotechnol 16:95-118
28. Shiroki R, Poindexter NJ, Woodle ES, Hussain MS, Mohanakumar T, Scharp DW (1994) Human peripheral blood lymphocyte reconstituted severe combined immunodeficient (hu-PBL-SCID) mice. A model for human islet allograft rejection. Transplantation 57:1555-62
29. Gamblin AL, Brennan MA, Renaud A, Yagita H, Lézot F, Heymann D, Trichet V, Layrolle P (2014) Bone tissue formation with human mesenchymal stem cells and biphasic calcium phosphate ceramics: The local implication of osteoclasts and macrophages, Biomaterials 34:9660-9667. doi: 10.1016/j.biomaterials.2014.08.018
30. Xia TS, Wang GZ, Ding Q, Liu XA, Zhou WB, Zhang YF, Zha XM, Du Q, Ni XJ, Wang J, Miao SY, Wang S (2012) Bone metastasis in a novel breast cancer mouse model containing human breast and human bone, Breast Cancer Res Treat 132:471-486. doi: 10.1007/s10549-011-1496-0
31. Holen I, Nutter F, Wilkinson JM, Evans CA, Avgoustou P, Ottewell PD (2015) Human breast cancer bone metastasis in vitro and in vivo: a novel 3D model system for studies of tumour cell-bone cell interactions, Clin Exp Metastasis 32:689-702. doi: 10.1007/s10585-015-9737-y
32. Hildebrand T, Laib A, Müller R, Dequeker J, Rüegsegger P (1999) Direct three-dimensional morphometric analysis of human cancellous bone: microstructural data from spine, femur, iliac crest, and calcaneus. J Bone Miner Res. Jul;14(7):1167-74.
33. Tong X, Burton IS, Jurvelin JS, Isaksson H, Kröger H (2016) Iliac crest histomorphometry and skeletal heterogeneity in men.Bone Rep. Nov 28;6:9-16. doi: 10.1016/j.bonr.2016.11.004.